LWT - Food Science and Technology 154 (2022) 112797

Contents lists available at ScienceDirect

LWT

journal homepage: www.elsevier.com/locate/lwt

Micro-dispersed essential oils loaded gelatin hydrogels with antibacterial activity

Thomas B. Goudoulas [a,d], Sonja Vanderhaeghen [b], Natalie Germann [a,c,*]

[a] Fluid Dynamics of Complex Biosystems, TUM School of Life Sciences, Technical University of Munich, Maximus-von-Imhof-Forum 2, 85354, Freising, Germany
[b] Chair of Microbiology, TUM School of Life Sciences, Technical University of Munich, Emil-Ramann-Str. 4, 85354, Freising, Germany
[c] Fluid Mechanics, Department of Chemical and Biochemical Engineering, Technical University of Dortmund, Emil-Figge-Str. 68, 44173, Dortmund, Germany
[d] Brewing and Beverage Technology, TUM School of Life Sciences, Technical University of Munich, Maximus-von-Imhof-Forum 2, 85354 Freising, Germany

ARTICLE INFO

Keywords:
Gelatin
Essential oils
Hydrogels
Viscoelastic properties
Antibacterial activity

ABSTRACT

Plant-based essential oils (EOs) are natural antimicrobial agents that have a relatively new application as edible coatings to extend the shelf life of foods such as meat. In this study, we developed gelatin hydrogels containing microdroplets of rosemary essential oil (REO) and orange essential oil (OEO). The microdroplets were successfully stabilized by the surfactant Tween®80. The droplet size distribution was slightly affected by the type of EO and homogenization time. The rheological properties in the linear viscoelastic range depend on the EO concentration and the Bloom number of the gelatin. The nonlinear behavior remains typical of gelatin gels, with stiffening and shear thickening at large deformation amplitudes. *Escherichia coli* and *Bacillus cereus* were sensitive to the gelatin-REO hydrogels with a minimum inhibitory concentration (MIC) of 0.5%. The gelatin-OEO hydrogels inhibited only *Bacillus cereus* with an MIC of 0.5%, but the gelatin-REO hydrogels showed greater cell reduction. Surprisingly, the *Staphylococcus aureus* strain used here was resistant to all gelatin-EO hydrogels. Our experiments show that gelatin-EO hydrogels prepared by simple emulsification have high stability and antibacterial activity suitable for potential preservation of gelatin-tolerant foods.

1. Introduction

Gelatin is an amphiphilic biopolymer that is soluble in water above 35 °C, i.e., close to body temperature, a fundamental feature of many food applications (Dille, Hattrem, & Draget, 2018). Below this temperature, it gradually reverts to a triple helix structure (Taylor, Tomlins, & Sahota, 2017). At a given temperature, the concentration and Bloom number of gelatin mainly determine the sol-gel and gel-sol transitions (Goudoulas & Germann, 2017; Joly-Duhamel, Hellio, Ajdari, & Djabourov, 2002; Netter, Goudoulas, & Germann, 2020). During gelation, the molecular conformation changes from random coils to helices stabilized by hydrogen bonds. The number of helices directly correlates with the storage modulus, an essential parameter for gelatin hydrogels determined by oscillatory shear measurements (Eysturskard, Haug, Ulset, & Draget, 2009; Joly-Duhamel et al., 2002).

Essential oils (EOs) are increasingly used as food flavorings and additives due to their excellent antibacterial and antimicrobial activity (Butnariu & Bostan, 2011; Muthaiyan, Biswas, Crandall, Wilkinson, & Ricke, 2012). However, in the particular case of plant extracts, adverse effects and risks may occur (Salehi, Sharopov, Tumer, Cho, & Martins, 2019). Rosemary oil (REO) and orange oil (OEO) have validated antimicrobial activity (Deans & Ritchie, 1987). The phenolic compounds carnosic acid and carnosol enhance the antimicrobial activity of REO, mainly by disrupting the cell membrane (Sikkema, De Bont, & Poolman, 1995; Tongnuanchan & Benjakul, 2014). The activity of OEO is based on limonene (Yashaswini & Arvind, 2018). The antibacterial activity can be tested with food contaminants such as *Escherichia coli (E. coli)*, *Staphylococcus aureus (S. aureus)*, and *Bacillus cereus (B. cereus)*. *E. coli*, a commensal Gram-negative bacterium in the human gut, can contaminate meat products and cause severe illness (de Assis et al., 2020). The gram-positive *S. aureus* is a commensal of human skin flora that can produce heat-stable enterotoxins after contaminating foods such as milk or meat (Cenci-Goga, Karama, Rossitto, Morgante, & Cullor, 2003). *B. cereus* is a Gram-positive contaminant of vegetables and starchy foods. The formation of heat-resistant endospores is a serious problem for restaurants and caterers because *B. cereus* enterotoxins cause diarrhea

* Corresponding author. Fluid Dynamics of Complex Biosystems, TUM School of Life Sciences, Technical University of Munich, Maximus-von-Imhof-Forum 2, 85354, Freising, Germany.
E-mail address: natalie.germann@tu-dortmund.de (N. Germann).

https://doi.org/10.1016/j.lwt.2021.112797
Received 17 June 2021; Received in revised form 18 October 2021; Accepted 7 November 2021
Available online 10 November 2021

(Osimani, Aquilanti, & Clementi, 2018).

Various EOs have been embedded in edible films, gelatin coatings, and other biopolymers for flavoring, packaging, and product preservation (Acevedo-Fani, Salvia-Trujillo, Rojas-Graü, & Martín-Belloso, 2015; Atares & Chiralt, 2016). Recently, hydrophobic or hydrophilic surfactants with aqueous solutions of fish gelatin were used to prepare edible films (Li, Tu, Sha, Ye, & Li, 2020). The preparation of stable oil droplets as bioactive compounds is not easy in aqueous gelatin solutions due to droplet aggregation (Paulo, Alvim, Reineccius, & Prata, 2020; Zhang, Ding, Wang, & Zhong, 2020). Therefore, surfactants are needed to stabilize the dispersed phase in emulsions (Kim, Beak, & Song, 2018). Gelatin hydrogels melt rapidly after oral ingestion at body temperature to accelerate the release of bioactive and flavoring ingredients (Dille et al., 2018). Understanding the mechanical behavior of hydrogels under large deformation is necessary because such conditions approximate food processing or chewing in the mouth (Sun, Huang, Yang, Liu, & Tong, 2015). Although edible gelatin-EO dry films have been studied in the last decade, systematic knowledge on EOs microdispersed in gelatin hydrogels is still limited.

The present study aims at a novel application of gelatin-EO hydrogels in food technology. The composition of the filled hydrogels is varied by considering two gelatin Bloom numbers of 100 and 240 and two different types of EOs, namely ROE and OEO. We evaluate the linear and nonlinear viscoelastic behavior of the gels in a wide range of deformations, as such information is essential for optimal food processing. Further, we investigate the antibacterial effect of the gels on Gram-negative and Gram-positive bacteria. The scope of the present study is a fundamental first step to identify future applications of microdispersed EO loaded hydrogels as coatings for meat products and validate longer food shelf life.

2. Materials and methods

2.1. Materials

Reinert Ingredients GmbH, Germany, kindly provided porcine gelatin (type A) with Bloom numbers 100 and 240. Netter et al. (2020) give details on the molecular weight of these gelatin batches. OEO (Item No. 3803.1, density = 0.85 g/cm^3) and REO (Item No. 3336.2, density = 0.91 g/cm^3) were purchased from Carl Roth GmbH, Germany. The surfactant Tween® 80 was purchased from Sigma-Aldrich Chemie GmbH, Germany. The surface tension of the EO droplets in air was measured using a KRÜSS system (Germany) and Drop Shape software (KRÜSS Advance 1.6.2.0). The surface tension of OEO and REO was 18.72 ± 1.5 mN/m and 16.02 ± 1.01 mN/m, respectively.

2.2. Preparation of emulsions and filled gels

Deionized water was used as the aqueous starting phase for all samples to dissolve gelatin at 3 wt%. The solution was gently stirred for 45 min at 45 °C in a water bath. Tween® 80 was added at a weight ratio of 1:1 to the EO content, similar to the protocol described by Li et al. (2020). The mixture was stirred for 15 min. This surfactant has been previously used in various EO emulsions (Fathi-Achachlouei, Babolanimogadam, & Zahedi, 2021; Wu et al., 2015; Zhang, Ding, Tao, Wang, & Zhong, 2020). The prepared mixtures were transported in 50-ml Falcon-type tubes and cooled at room temperature. Then, the EO was added with a precision micropipette on an analytical balance (Shimadzu, AUW220D, Shimadzu Scientific Instruments) at concentrations of 0.25, 0.5, and 1 wt%. A VDI 12 homogenizer (VWR, Germany) with a 512N-125 dispersing element was used at a speed of 8000 rpm for 60 s. In the preliminary experiments, the homogenization time was varied between 45 and 90 s to determine the effects of droplet size distribution. Finally, the EO-in-water emulsions were stored and gelified at 6 ± 1 °C.

2.3. Characterization of gelatin-EO emulsions

2.3.1. Determination of droplet size distribution (DSD)

The DSDs of the EOs were determined by laser diffraction using a dual wavelength detection system (Mastersizer Hydro 2000S, Malvern Instruments). The obscuration values were >5 to achieve an acceptable signal-to-noise ratio and good reproducibility. The refractive index of the dispersed oil phase was 1.468, similar to the EO value reported by (Rodríguez-Rojo, Varona, Núñez, & Cocero, 2012). The characteristic droplet sizes reported here are 10, 50, and 90% of the volume-based DSD, and d3/2 and d4/3 as area-weighted and volume-weighted mean diameters, respectively. The sizes given are the average of three measurements.

2.3.2. Stability evaluation

The physical stability of the emulsions was analyzed after the initial preparation and repeated liquefaction of the gels. Droplet migration phenomena were recorded as a function of time using a Turbiscan Classic MA2000 (Formulaction, France) by analyzing the variation of backscatter profiles for all EOs and concentrations. Transmission and backscatter data were collected every 40 μm at a maximum height of 80 mm of the measurement cuvette. The percentage intensity of backscattered light and the height of the sample determined destabilization. Each gelatin-EO batch was stored at 35 °C with gentle agitation before being transported to the measurement cuvette.

2.3.3. Optical microscopy

The DM4000M light microscope (Leica Microsystems IR GmbH, Germany) with its associated digital camera and software was used to assess the morphology and distribution of the droplets. Images were acquired with 20× and 40× objectives. For this purpose, 10 μl of the liquid emulsion sample was placed on slides without coverslips to avoid droplet compression.

2.4. Rheological characterization of gelatin-EO hydrogels

Prior to each rheometric measurement, a complete phase transition (gel-sol) was achieved in a water bath at a temperature of 45 ± 1 °C for at least 20 min. Depending on the distance between the parallel plates, 1.6–2.3 ml of the gelatin-EO-sol sample was used. *In situ* gelation was performed according to the procedure described in Netter et al. (2020). The temperature was lowered from the initial temperature of 35 °C to the gelation temperature of 5 °C, and the samples rested for 30 min to obtain the hydrogels. Unlike the pure gelatin-sol samples, the gelatin-EO-sol samples spread on the bottom plate due to the surfactant. Therefore, the horizontal alignment of the rheometer must be precise with a fast gap adjustment.

The rheometric measurements were performed on the hydrogels using the Kinexus Ultra+ rheometer equipped with the rSpace® software (NETZSCH GmbH, Germany). A parallel plate geometry of 50 mm diameter was used, and the gap was varied between 0.6 and 1.8 mm. Initial preliminary measurements were performed with a smooth upper plate. The roughness of the lower plate was 5.3 μm. A sandpaper with an average roughness of 18.7 μm (Grit P320, Waterproof, Norton Abrasives-St. Gobain) was bonded to the upper plate to prevent slippage during large amplitude oscillatory shear (LAOS) measurements. A removable hood over the sample, surrounded by a water-filled rim, was used to prevent sample evaporation. Strain sweep measurements were performed at 5 °C for strain amplitudes (γ) from 0.1 up to 1000%. The nonlinear LAOS experiment provides extensive data on the material structure, processing, and application of gelatin gels (Goudoulas & Germann, 2017; Netter et al., 2020; Sun et al., 2015). The angular frequency (ω) was 1 rad/s. All measurements were performed in triplicate on fresh samples.

2.5. Antibacterial activity of gelatin-EO hydrogels

2.5.1. Bacterial strains and culture conditions

We tested the antibacterial activity of gelatin-EO hydrogels with the Gram-negative *E.coli* strain DSM 30083T (Deutsche Sammlung von Mikroorganismen und Zellkulturen GmbH, Germany) (DSMZ) and the Gram-positive bacteria *S. aureus* Copenhagen DSM 20232 (DSMZ) and *B. cereus* (self-isolation 1996, Department of Microbiology, Technical University of Munich). Since the taxonomy of the B. *cereus* group is constantly changing (Liu et al., 2015), the 16S rRNA isolate was amplified with standard primers (27F AGAGTTGATCMTGGCTCAG, 1492R CGGTTACCTTGTTACGACTT; Lane, 1991) and Q5 polymerase (New England Biolabs, USA). Sanger sequencing was performed by Genewiz (USA). The *B. cereus* isolate had 99% 16S rRNA sequence similarity to *B. cereus*, confirming the species. Cultures for all antibacterial experiments were grown overnight by shaking (180 rpm) in 100 ml Erlenmeyer flasks and in 20 ml Lysogeny Broth Medium (LB, Bertani 1951) containing 3% NaCl (LB-NaCl, 10 g tryptone, 5 g yeast extract, 30 g sodium chloride, pH 6.5. All chemicals were purchased from Carl Roth GmbH, Germany). *E. coli* and *S. aureus* were incubated at 37 °C and *B. cereus* at 30 °C.

2.5.2. Plate assays for antimicrobial activity tests of gelatin-EO hydrogels

For the antimicrobial assays, a specific number of bacteria were plated and covered with a gelatin sheet. After incubation at various time points, the plate contents were homogenized and plated for overnight culture. The number of colonies grown per ml initial volume of cells (colony forming units/ml, cfu/ml) is a measure of the comparison of bacteria that survived after contact with the gelatin-EO hydrogels. For each of the plating tests, 9 g of LB-NaCl solid medium (15 g/l agar-agar; Carl Roth GmbH, Germany) was prepared in Petri dishes (5 cm diameter). The initial cfu/ml used for plating *E. coli* was $4.1{\cdot}10^7$ cfu/ml and that of S. *aureus* was $1{\cdot}10^7$ cfu/ml. *B. cereus* formed aggregates in the liquid culture (Supplementary Information file, Fig. S.5) and prevented the formation of individual colonies. For separation, the entire preculture was gently sonicated with a Hielscher UP200S instrument (10 s, 20% amplitude, 0.25 cycles, Schneiderheinze, Armstrong, Schulte, & Westenberg, 2000) before plating at a cell count of $1{\cdot}10^8$ cfu/ml. In initial experiments, we determined a balance between cell separation and cell death. However, less aggressive methods such as adding triphenyltetrazolium chloride to the medium could improve the results (Vardanian, Kurzbaum, Farber, Butnariu, & Armon, 2017). Plates containing one of the bacterial species were dried. Then, 1 ml of gelatin hydrogels (3 wt% gelatin, Bloom 100), melted at 37 °C, was poured onto the plates and solidified at 4 °C. Pure gelatin and emulsions containing 0.25, 0.5, and 1 wt% REO and 0.5 and 1 wt% OEO were tested.

After incubation of the plates for 2, 4 or 6 h at 16 °C, all LB-NaCl solid medium including bacteria and hydrogel was filled with 90 ml phosphate buffer (8 g/l NaCl, 0.2 g/l KCl, 1.44 g/l Na2HPO4, 0.24 g/l KH2PO4, pH 7.4) in 400 ml poly silk bags (BagLight® Interscience, France) and homogenized in a Stomacher lab-blender 400 (Gemini BV, The Netherlands) for 2 min. Subsequently, 100 μl of the homogenate was applied to solid LB medium (9 cm diameter Petri dishes) and incubated at growth temperature for 14 h. The assay was performed in biological triplicates and technical replicates. Finally, colonies were counted and cfu/ml values were calculated. Two-tailed paired Student's t-tests show significant growth differences between incubation with gelatin or emulsions (Microsoft Excel, p-value < 0.05).

2.5.3. Microscopic evaluation of bacteria

E. coli, *S. aureus*, or *B. cereus* precultures were mixed 1:1 with LB medium, gelatin, or gelatin emulsions (1 wt% REO, 1 wt% OEO) and incubated at 37 °C. Samples were collected at 30 min intervals for 2 h (0, 30, 60, 90, and 120 min). An Axio Imager M1 microscope with ZEN 3.0 software (Zeiss, Germany) examined *B. cereus* and *S. aureus* in two and *E. coli* in three biological replicates. Aggregate size and cell number of *E. coli* were determined using ImageJ (Schneider, Rasband, & Eliceiri, 2012). Boxplots of *E. coli* aggregate sizes and ANOVA tests were performed using R software i386 4.0.3 (R Core Team, 2020). The ANOVA test was significant at a p value < 0.05.

3. Results and discussion

3.1. Characterization of gelatin-EO emulsions

The DSDs of the microdroplets in aqueous gelatin were measured for different homogenization conditions and EO concentrations. The results in Fig. 1 confirm that the droplet size decreases with increasing homogenization time. A short homogenization time of 45 s leads to bimodal distributions. The differences between the two types of EOs can be explained by the equilibrium surface tension values and the shear and mixing conditions in the homogenization tube. As the homogenization time increases, the number of larger droplets decreases significantly. At lower EO concentrations, a broader size distribution is formed, a common observation for both EOs. Table 1 lists the characteristic sizes for the emulsions produced at 8000 rpm for 60 s. Our d_{50} values are in agreement with the REO results of Rodríguez-Rojo et al. (2012) obtained on the first day after emulsification. From Fig. 1 and Table 1, we conclude that 60 s of homogenization is sufficient to generate emulsions with unimodal and narrow DSDs.

Microscopy images show the morphology and size estimation of the EO droplets. Fig. 2 shows representative cases with spherical droplets. In the SI file, see Sec. S.4 for a detailed discussion of the morphology and parameters affecting droplet formation (surfactant, homogenization time, and rotation speed). At this point, brief mention should be made of the effect of Tween® 80, as this nonionic hydrophilic surfactant has a large volume ratio between hydrophilic head and hydrophobic tail, and such a high ratio leads to greater droplet curvature (Zhang, Ding, Tao, et al., 2020).

The emulsions were stable during heating and cooling between 40 °C and refrigerator conditions. Fig. 3 shows backscatter profiles as a function of cell height for different time points after liquefaction. The data in Fig. 2B show that the homogeneity of the emulsion is constant above 8 mm, with a significant stable backscatter profile for about 2 h. A small increase occurs at 104.15 min (cyan, orange and green curves) above 67 mm, i.e., at the top of the measurement cell. The behavior of the sample in Fig. 2A is similar, with varying intensity. The results indicate that in the *in situ* rheological gelation study, i.e., during the 30-min temperature reduction to bring the sample to 5 °C, creaming is negligible. At 5 °C, rapid gelation occurs, which hinders the movement of the droplets. In the Supplementary Information (SI) file, Fig. S.2 shows the corresponding backscatter profiles for the gelatin-OEO emulsions. For these samples, almost all curves agree above 12 mm. Again, Fig. S.2 indicates stable emulsions up to 2 h, as it shows repeatable and stable profiles from the center to the top of the cell.

3.2. Rheology of gelatin-EO hydrogels

Fig. 4 shows examples of typical strain measurements on a 3 wt% gelatin gel. The data were obtained with smooth surface geometries. The dispersed EO has no effect on the LAOS response, which is similar to that reported by Netter et al. (2020) for pure gelatin. Therefore, a more elastic gel is observed for the higher Bloom number. In both cases, significant nonlinear stiffening behavior precedes the rapid yielding that occurs after the maximum stiffening (between 100 and 200% strain amplitude). The average values of the elastic and viscous moduli, G' and G'', respectively, at each strain point are shown in the following graphs. A detailed plot and discussion of hydrogel yielding can be found in the SI file in Sec. S.3. Overall, the nonlinear response prior to yielding is attributed to the stiffening within the cycle, which is not affected by the microdroplets.

In Fig. 5, viscoelastic data from strain sweeps are presented to show

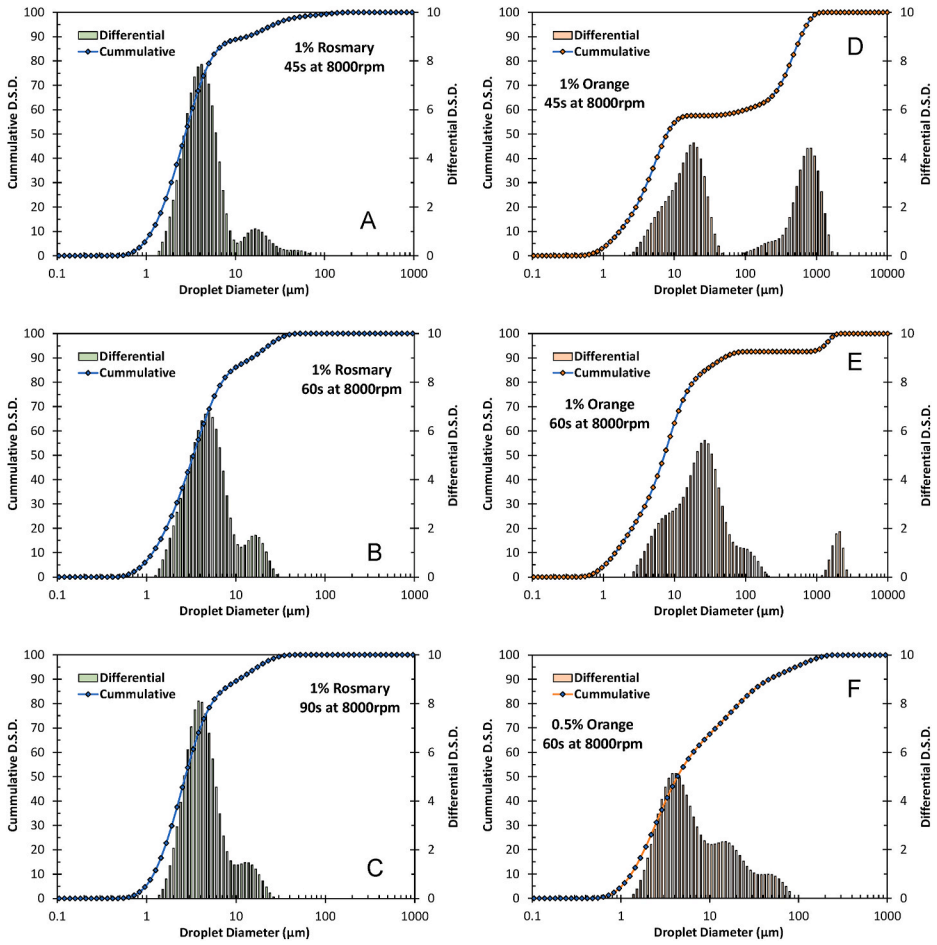

Fig. 1. Droplet size distribution (DSD) of gelatin-EO emulsions for different conditions. The column on the left side refers to REO at different homogenization times (A to C), while the right side shows the effects of concentration and two homogenization times (D to F) for OEO.

Table 1
Characteristic droplet sizes for the emulsions used in the preparation of gelatin-EO gels.

	d_{10}	d_{50}	d_{90}	$d_{3/2}$	$d_{4/3}$
Orange 0.5 wt%	1.307	4.332	46.755	3.097	17.55
Orange 1 wt%	1.475	7.194	49.245	3.885	113.93
Rosemary 0.5 wt%	1.328	4.043	84.87	3.149	35.61
Rosemary 1 wt%	1.165	3.38	14.76	2.507	5.838

details from the nonlinear region. The total rheological response is given as dimensionless ratios to an initial value in the linear viscoelastic range. The reference values chosen are 0.1% strain amplitude, far from the nonlinear response. The main interest is the strain-stiffening and shear-thickening upturns of G′ and G″, respectively, together with the successive yielding. Such a representation clearly shows the nonlinear behavior, although the actual magnitude of the elastic and viscous moduli disappears. The gelatin-REO hydrogel exhibits a slightly higher stiffness than the gelatin-OEO hydrogel. However, the striking difference is the much higher shear thickening peak. This could be related to the fact that the OEO penetrates the gel mass with relatively larger oil droplets and the energy dissipation increases accordingly during the deformation of the gel matrix. As for the critical strain amplitudes, the flow behavior (sharp decrease of G′) and shear thickening peak (maximum of G″) are comparable for both EOs. The shift of G″ from the critical strain to higher values is similar to that described for a comparable gelatin concentration of 3 wt% (Goudoulas & Germann, 2019; Netter et al., 2020).

Finally, we compare pure gelatin with the gelatin-EO hydrogels. Pure gelatin forms a homogeneous gel structure as it does not contain any additives or droplets. In pure gelatin, no physical interaction between oil droplets is observed, resulting in a structural reinforcement of the gelatin network. In gelatin-EO hydrogels, the surfactant could displace the gelatin molecules from the oil-water interface. As a result, the oil droplets acted as inactive fillers that reduced the elastic behavior (Dille et al., 2018). Fig. 6A shows that for 240 Bloom, the pure gelatin gel differs from the gelatin-EO hydrogels. Pure gelatin exhibits a higher stiffening value than orange and rosemary gels. However, the difference in size is small, indicating that the EOs only slightly affect the nonlinear mechanical behavior in the LAOS region. In contrast, no clear trend in magnitude can be seen for 100 Bloom in Fig. 6B. In this case, shorter structural units occur during the development of the gel structure due to the lower molecular weight. The shorter triple helices and their bundles can withstand higher deformations. Thus, if the final application of the gel involves high deformation fields, the lower Bloom number is advantageous.

3.3. Antimicrobial activity of gelatin-EO hydrogels

Gram-negative *E. coli* and Gram-positive *S. aureus* and *B. cereus* were used to determine the antimicrobial activity of gelatin-EO hydrogels at 16 °C in alignment tests. To simulate solid food systems, an aw value of 0.98 and a low pH of 6.5 were used, similar to Acevedo-Fani et al. (2015). The cfu/ml were counted after growth (SI File Table S1.). The gelatin-EO hydrogels tested contained either REO or OEO. As controls, the plated bacteria were covered either with pure gelatin or not covered

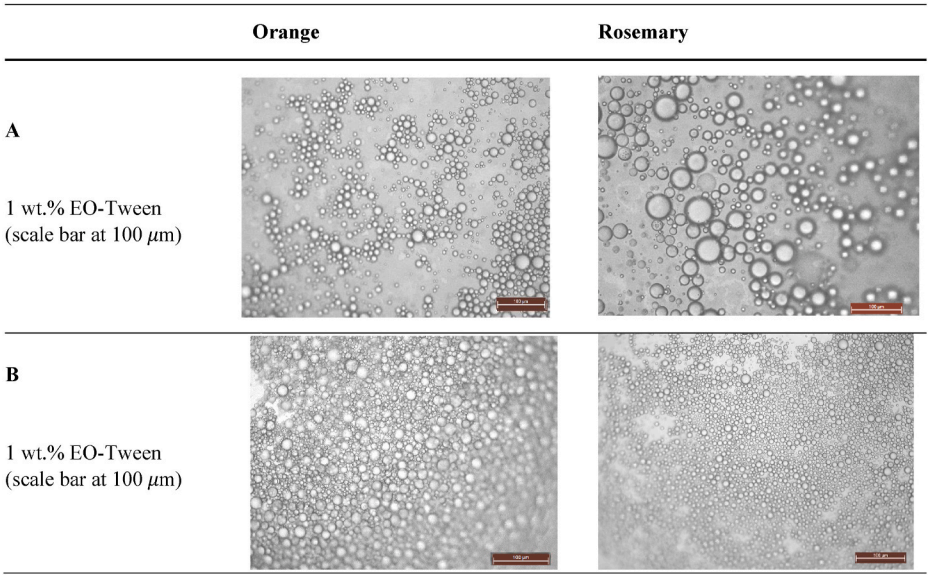

Fig. 2. Emulsions of **A:** 240 Bloom, and **B:** 100 Bloom for the corresponding two EOs. Homogenization speed and time: 8000 rpm and 60 s, respectively.

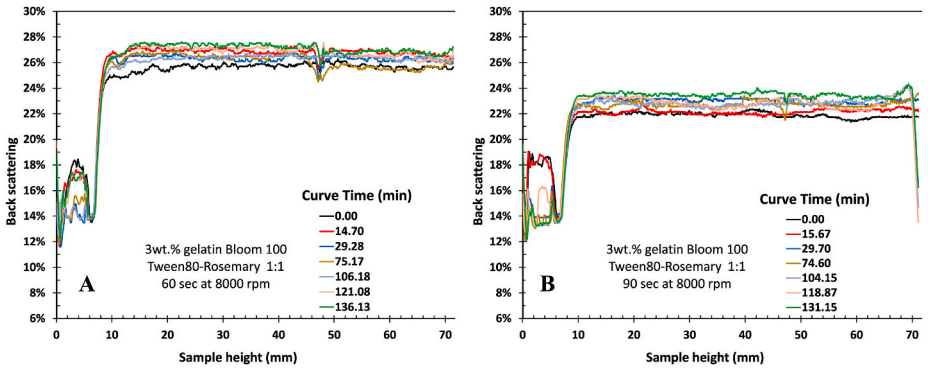

Fig. 3. Backscatter profiles of a 3 wt% gelatin-REO emulsion as a function of cell height for different times after liquefaction. Initial homogenization at 8000 rpm for **A:** 60 s and **B:** 90 s.

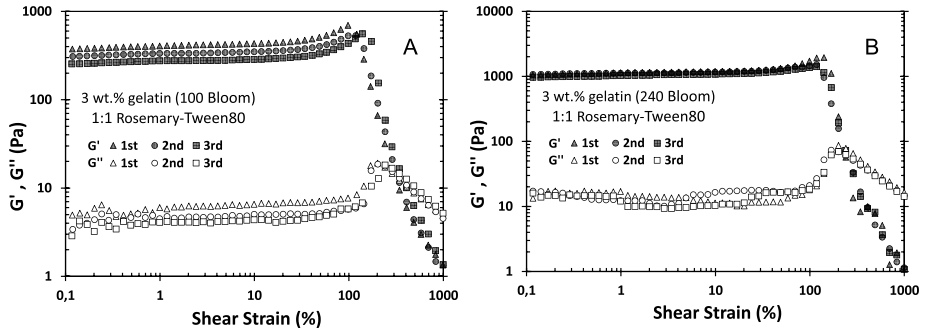

Fig. 4. Typical strain sweep measurements of different *in situ* gelatin gels filled with REO. The three measurements were performed on different samples from the same gelatin-REO batch. Data are for 1 wt% REO and gelatin containing **A:**100 Bloom and **B:** 240 Bloom.

with any gelatin hydrogel. The result of the comparison with the two controls showed that the gelatin did not affect bacterial growth (Fig. 7). The antibacterial effect started immediately within 2 h, which is consistent with the results of Acedevo-Fani et al. (2015).

3.3.1. *Antibacterial activity of gelatin-REO hydrogels*

The antibacterial activity of gelatin-REO hydrogels was tested with REO concentrations of 0.25, 0.5, and 1 wt%. This hydrogel had antibacterial activity in the following order: *S. aureus* < *E. coli* < *B. cereus* (Fig. 8). No significant effect was seen after incubation of *E. coli* with 0.25% REO (Fig. 7A). With increasing concentration, the inhibitory effect increased significantly. After incubation with 0.5 wt% REO, the average cfu/ml time ($8{\cdot}10^6$ cfu/ml) was lower than the gelatin-only control ($6{\cdot}10^7$ cfu/ml; p-value < 0.0006) by a $\log_{10}$ scale. The minimum inhibitory concentration (MIC) of REO on *E. coli* was 0.5 wt%. After incubation with 1% REO ($4{\cdot}10^5$ cfu/ml), cell reduction was lower

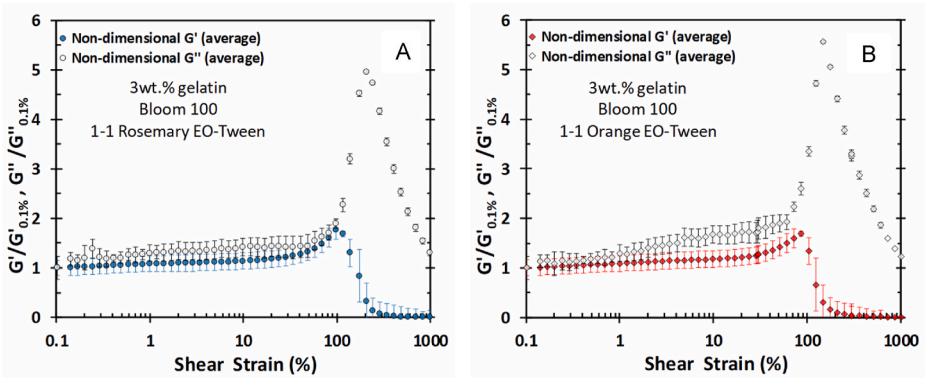

Fig. 5. Normalized strain sweeps for in-situ gelatin gels. The reference modulus values are at a strain amplitude of 0.1%. Data are from three different emulsion samples of the same batch: **A:** REO and **B:** OEO.

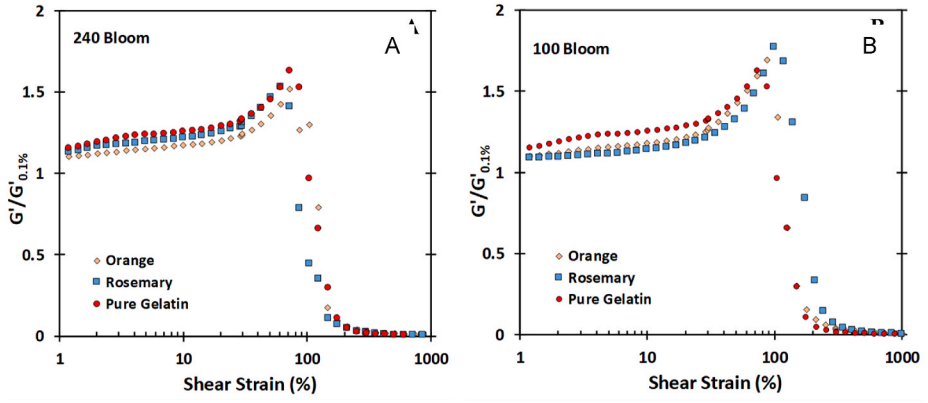

Fig. 6. Comparison of normalized strain sweeps for *in situ* pure gelatin and gelatin-EO gels. Standard deviation lines have been removed for clarity. Data are for 1 wt % EO and gelatin containing **A:**240 Bloom and **B:** 100 Bloom.

by a $\log_{10}$ scale than with 0.5 wt% REO (p-value < 0.0004). This result is consistent with the MIC of pure REO on *E. coli* determined by Burt (2004), which ranges from 4.5 to 10 μl/ml (1% (v/v) = 10 μl/ml). In contrast to previous studies testing the antibacterial activity of REO on *S. aureus* (Jafari-Sales & Pashazadeh, 2020; Nakagawa, Hillebrand, & Nunez, 2020), gelatin-REO hydrogels showed no antibacterial activity at the selected REO concentrations and incubation times tested (Fig. 7B). Other *S. aureus* strains may be more sensitive to gelatin-REO hydrogels than those used here. When *B. cereus* was incubated with gelatin-REO hydrogels, 0.5, and 1 wt% REO resulted in almost complete suppression of growth (Fig. 7C). The effect of 0.5 wt% REO was slightly less than that of 1 wt% REO. However, under both conditions, only a few colonies grew after plating. No growth inhibition was observed at 0.25 wt% REO, resulting in a MIC of 0.5 wt%. According to Burt (2004), the MIC of pure REO for *B. cereus* should be 0.2 μl/ml lower.

3.3.2. Antibacterial activity of gelatin-OEO hydrogels

The antibacterial activity of gelatin-OEO hydrogels was tested at the concentrations of 0.5 and 1 wt%. Whereas the gelatin-OEO hydrogels showed no effect on *E. coli* or *S. aureus* (Fig. 7. A and B), significant inhibition was found for *B. cereus* (Fig. 7. C). The effect is smaller than that of gelatin-REO hydrogels, in agreement with the work by Evrendilek (2015). The author tested the antimicrobial activity of orange peel oil compared to 13 other EOs such as anise, oregano, and mint and found that OEO had the lowest inhibitory effect on all tested bacteria. Non-confluent growth of *B. cereus* on some plates observed only after incubation with 0.5 wt% OEO hydrogel (SI file, Figs. S5 A - C) could be explained by a persistent effect of EO on *B. cereus* after plating the homogenized agar-bacteria-gelatin mixture. Small particles may still be present that were not evenly distributed during plating. This was not observed in *E. coli* where the agar-bacteria-gelatin mixture was diluted before plating (SI file, Fig. S5 D). The result affects the comparability of the plating tests for *B. cereus* incubated with 0.5 wt% OEO hydrogels. Such artifacts can be avoided by using adapted disk diffusion assays (Butnariu & Bostan, 2011), which are more established and have higher throughput than the method used here, but also do not allow for a time-dependent assay. Compared to Gram-negative *E. coli* on gelatin-EO hydrogels, the higher sensitivity of Gram-positive *B. cereus* is consistent with most previously published data showing that Gram-positive bacteria are more sensitive to EOs than Gram-negative bacteria (Burt, 2004).

3.4. Gelatin-EO hydrogel interactions with bacteria

Light microscopy was used to study the interactions of gelatin-EO hydrogel emulsions with bacterial cells during the first 2 h of treatment. As controls, cells were mixed with pure gelatin or LB medium. The images of *E. coli* show that gelatin aggregated the cells, whereas no aggregates were visible in the LB control (Fig. 8A and B). Aggregation also occurred in gelatin-OEO and gelatin-REO hydrogels. Moreover, ~95% of *E. coli* cells were aggregated in gelatin (SI file, Table S.2.), ~89% in OEO, and ~86% in REO. The observation shows that droplets formed in gelatin-REO and gelatin-OEO hydrogels interact with the aggregates. Some droplets adhered with fewer cells, others with larger aggregates (Fig. 8C and D). Larger aggregates often surrounded droplets. The aggregate size was measured on all images taken every 30 min for 2 h (18–20 images per gelatin hydrogel). The aggregates in gelatin-OEO (56 ± 133 μm^2, p-value ≤ 0.035) and those in gelatin-REO (50 ± 97

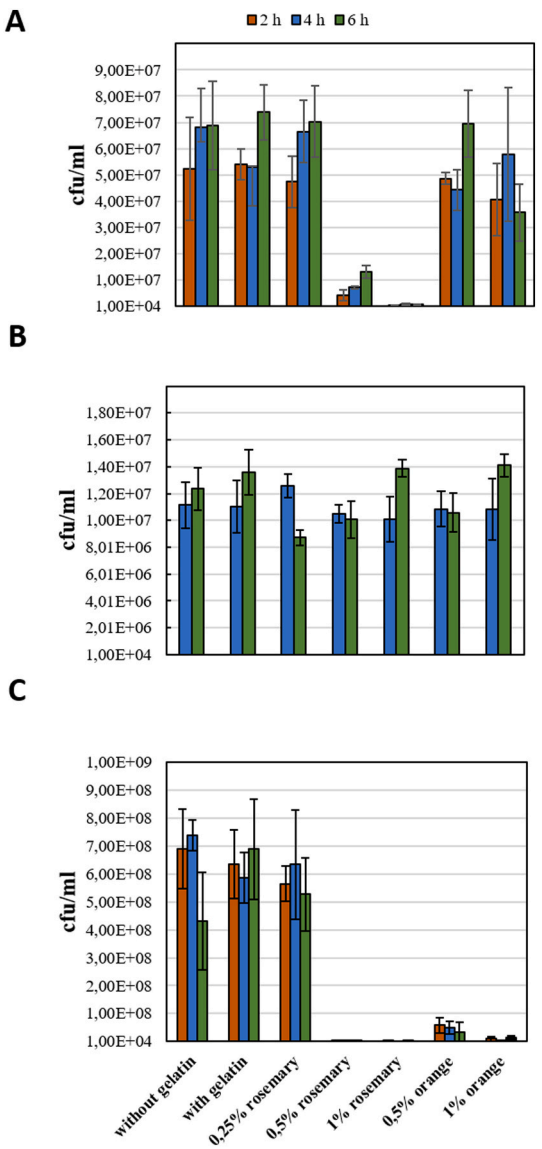

Fig. 7. Plate assays of **A**: *E. coli*, **B**: *S. aureus*, **C**: *B.cereus* to test the antimicrobial activity of gelatin-REO and gelatin-OEO hydrogels, respectively. Bacteria were incubated for 2 h (orange bars), 4 h (blue bars), or 6 h (green bars) with the gelatin hydrogels. REO was tested at concentrations of 0.25, 0.5, and 1 wt%. OEO was tested at concentrations of 0.5 and 1 wt%. The experiments were performed in three biological and two technical replicates. The colony forming units per ml (cfu/ml) were calculated. After incubation of the bacteria, the growth of a colony corresponds to 10^4 cfu/ml.

μm^2, p-value $\leq$ 0.020) were smaller than those in gelatin (119 $\pm$ 670 μm^2; SI file, Table S.3.). The aggregates in gelatin-OEO hydrogels disintegrated in the first 30 min of incubation, decreasing their size from 220 $\pm$ 344 μm^2 to 51 $\pm$ 57 μm^2 (SI file, Fig. S6; p-value $\leq 2.2 \cdot 10^{-16}$). Electrostatic interactions of bacteria with gelatin could explain these observations, as the cell surface of Gram-negative bacteria is more negatively charged than that of Gram-positive bacteria (Hong & Brown, 2008). However, we did not observe aggregation in Gram-positive bacteria. In this study, type A gelatin was used, i.e., acid extracted, resulting in a high isoelectric point (pI) of up to 9.4 (Poppe, 1992). Since we used a pH of about 6.5 in our experiments, the gelatin was positively charged. This could cause *E. coli* cells to bind to the gelatin, preventing homogeneous cell culture. Alternatively, *E. coli* pili could have caused the aggregation. They are formed during biofilm formation and allow attachment to surfaces or proteins, such as gelatin (Garnett et al., 2012). Unfortunately, no previous study has investigated the aggregation of *E. coli* in gelatin. We did not analyze this further in this work. Aggregation reduces the exposure of *E. coli* to the EO and thus may reduce the antimicrobial effect. This could be prevented by using a different, less acidic type of gelatin. Regarding the lack of effect of gelatin-EO hydrogels on *S. aureus*, microscope images showed that gelatin hydrogels did not change the morphology of this bacterium (Fig. 9).

From the microscope images, it is clear that *B. cereus* was present as single cells or aggregated in liquid cultures (SI file, Fig. S7). However, gelatin and gelatin-EO hydrogels had no effect on aggregation (Fig. 10). Cell morphology did not change after incubation with pure gelatin (Fig. 10A and B) and gelatin-OEO (Fig. 10C and D). However, cell morphology changed after incubation with gelatin-REO hydrogels for 1 h (Fig. 10E and F). The rods had a smooth surface at the beginning and later became wrinkled. As reported in one study, antimicrobial components of REO can penetrate the membrane (Ojeda-Sana, van Baren, Elechosa, Juárez, & Moreno, 2013), which could explain the wrinkled morphology of *B. cereus*. The osmotic effect of NaCl could enhance this effect (Marquis, 1968). Fu et al. (2007) confirmed that a low REO concentration on the surface of *Propionibacterium acnes* increased the cell surface area without changing the length of the bacteria. A similar change in the cell surface was observed for *B. cereus*, but the cell size remained unchanged. The light microscopy used here shows only gross cell shapes, but other studies confirmed the change in cell structure after exposure to EOs by electron microscopy (Alizadeh Behbahani, Noshad, & Falah, 2019).

Under *in vitro* conditions, the tested antimicrobial activity of edible films was reported to change when used in food due to the complex food composition (Weiss, Loeffler, & Terjung, 2015). However, gelatin films containing EOs successfully increased the shelf life of chicken fillets (Fanthi-Achachlouei, Babolanimogadam, & Zahedi, 2020). For example, chicken fillets coated with gelatin anise oil were still edible after 12 days of storage after the fillets were inoculated with Gram-positive or Gram-negative bacteria, yeasts, or molds. In contrast, controls spoiled after six days. In conclusion, the first antimicrobial results using dispersed microdroplets of REO or OEO on the food contaminants *E. coli* and *B. cereus* were successful. The morphology of the bacteria changed after direct mixing with the gelatin-OEO emulsions. However, we do not know the morphological effect of the gelatin film to which the bacteria grown on the surfaces are exposed. For a possible application as a coating for meat products, it is crucial to test the corresponding gels with meat products to verify a longer shelf life of the food.

4. Conclusions

In this study, we investigated the mechanical properties of gel matrices made of gelatin filled with microdroplets of REO and OEO obtained by simple emulsification. In addition, the antibacterial properties of these gels against the food contaminants *E. coli, S. aureus*, and *B. cereus* were determined. Under the particular conditions of preparation of the emulsions, the average sizes of the DSD were up to 10 μm. The main viscoelastic behavior of the filled gels remained qualitatively the same, with demonstrated stiffening and shear thickening behavior. These properties are important because the gel must remain intact during industrial processing and the sensory properties should be affected during oral chewing as a bulk product.

We also systematically performed *in-vitro* antimicrobial tests at relatively low temperatures where the bacteria were still active. The strongest antibacterial effect was observed with *B. cereus*, which was also evident from the wrinkled morphology of the cells exposed to the gelatin-EO hydrogels. The growth of *E. coli* was less inhibited, while *S. aureus* was completely unaffected. Surprisingly, *E. coli* cells aggregated even after mixing with pure gelatin, which can be explained by electrostatic interactions. We obtained high stability and considerable antibacterial activity, making such hydrogels suitable for future use in edible coatings of perishable foods such as meat. As edible films

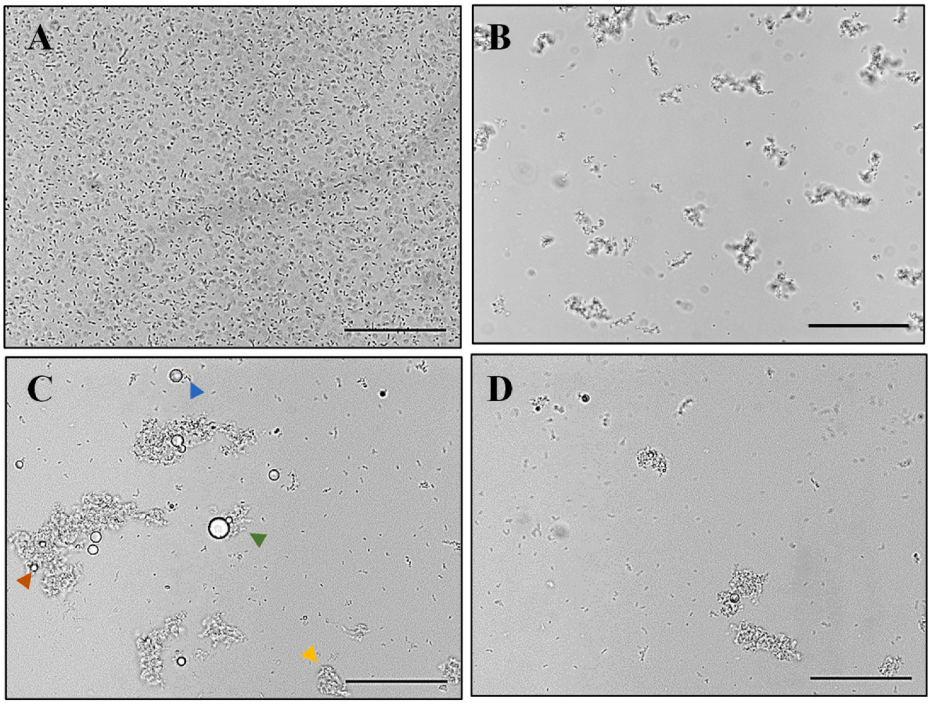

Fig. 8. *E. coli* incubated on **A:** pure LB medium**, B:** gelatin**, C:** LB + gelatin +1 wt% OEO**, D:** LB + gelatin +1 wt% REO. The pictures were taken with a 40× objective (scale bar 20 μm). Arrows in **C** show EO droplets embedded in aggregates (orange), EO droplets with few cells (blue), EO droplets associated with bigger aggregates (green), or aggregates without EO droplets (yellow). A culture with ~$1.6{\cdot}10^8$ cells/ml of *E. coli* was mixed 1:1 with each agent. Experiments were performed in three biological replicates taking two representative pictures at each time point.

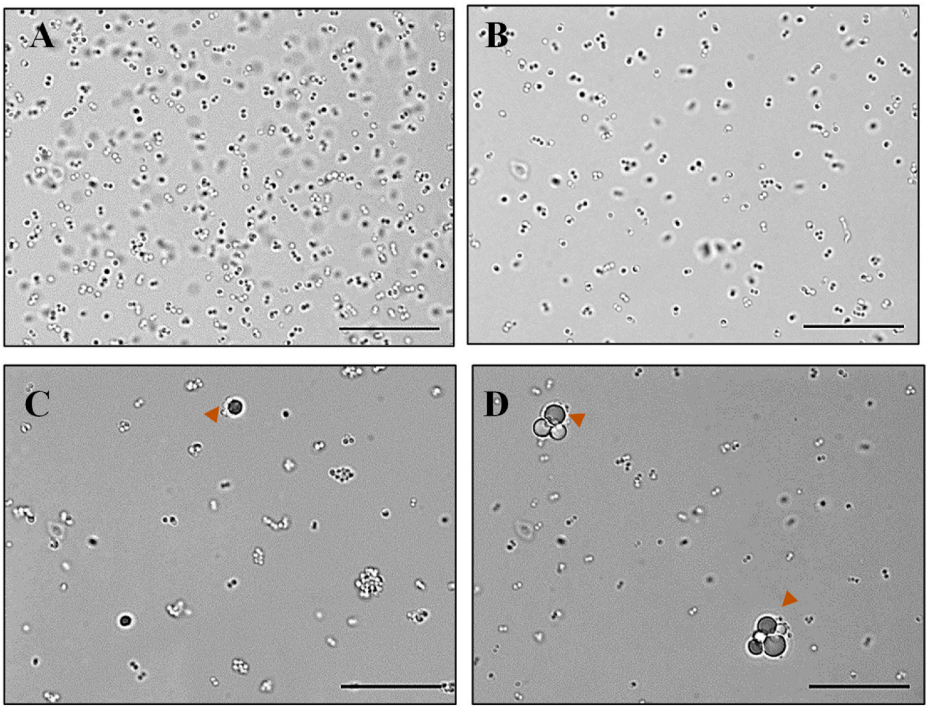

Fig. 9. *S. aureus* incubated with **A:** LB medium**, B:** gelatin**, C:** gelatin +1 wt% OEO**, D:** gelatin +1 wt% REO. The pictures were taken with a 100× objective (scale bar 50 μm). Arrows in **C** and **D** show EO-droplets associated with few cells. A culture with ~$1.5{\cdot}10^9$ cells/ml of *S. aureus* was mixed 1:1 with each agent. Experiments were performed in three biological replicates taking two representative pictures at each time point.

containing plant-derived EOs have become the focus of interest, micro-dispersed EO loaded hydrogels may find interesting applications in low-calorie and low-fat meat products in the future.

CRediT authorship contribution statement

Thomas B. Goudoulas: Data curation, Conceptualization, Methodology, Investigation, Validation, Visualization, Writing – original draft, preparation, Writing – review & editing. **Sonja Vanderhaeghen:** Data curation, Methodology, Investigation, Validation, Formal analysis, Visualization, Writing – original draft, preparation, Writing – review & editing. **Natalie Germann:** Supervision, Conceptualization, Methodology, Validation, Writing – review & editing, Funding acquisition.

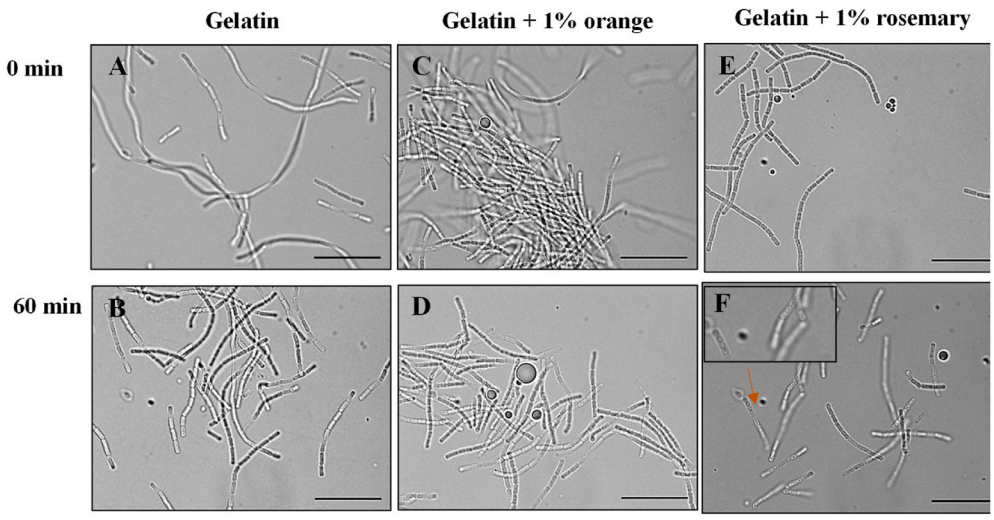

Fig. 10. *Bacillus cereus* after mixing with gelatin, gelatin +1 wt% OEO, or gelatin +1 wt% REO (A, C, E) and after 60 min incubation with the respective agent (B, D, F). Images were taken with a 100× objective (scale bar 50 μm). The orange arrow in **F** elucidates the shriveled cells after incubation with gelatin +1 wt% REO. A culture with ~$3{\cdot}10^7$ cells/ml of *B. cereus* was mixed 1:1 with each agent. Experiments were performed in three biological replicates taking two representative pictures at each time point.

Declaration of competing interest

None.

Acknowledgment

The work was supported by Allianz Industrie Forschung [grant number ZF4025025SK7]. The authors thank the industrial cooperation partner Reinert Ingredients GmbH for the gelatin samples. Also, Prof. U. Kulozik and Dr. I. Kieferle for providing access to the Malvern Mastersizer 2000. The authors thank Prof. S. Scherer for providing the stomacher blender and Dr. N. Thieme for providing R scripts. Finally, the assistance of Ms. M. Uebelacker and Mr. Md. H. Sime with the laboratory work is acknowledged.

Appendix A. Supplementary data

Supplementary data to this article can be found online at https://doi.org/10.1016/j.lwt.2021.112797.

References

Acevedo-Fani, A., Salvia-Trujillo, L., Rojas-Graü, M. A., & Martín-Belloso, O. (2015). Edible films from essential-oil-loaded nanoemulsions: Physicochemical characterization and antimicrobial properties. *Food Hydrocolloids, 47*, 168–177. https://doi.org/10.1016/j.foodhyd.2015.01.032

Alizadeh Behbahani, B., Noshad, M., & Falah, F. (2019). Cumin essential oil: Phytochemical analysis, antimicrobial activity and investigation of its mechanism of action through scanning electron microscopy. *Microbial Pathogenesis, 136*, 103716. https://doi.org/10.1016/j.micpath.2019.103716

de Assis, D. C. S., da Silva, T. M. L., Brito, R. F., da Silva, L. C. G., Lima, W. G., & Brito, J. C. M. (2020). Shiga toxin-producing *Escherichia coli* (STEC) in bovine meat and meat products over the last 15 years in Brazil: A systematic review and meta-analysis. *Meat Science, 173*, 108394. https://doi.org/10.1016/j.meatsci.2020.108394

Atares, L., & Chiralt, A. (2016). Essential oils as additives in biodegradable films and coatings for active food packaging. *Trends in Food Science & Technology, 48*, 51–62. https://doi.org/10.1016/j.tifs.2015.12.001

Burt, S. (2004). Essential oils: Their antibacterial properties and potential applications in foods—a review. *International Journal of Food Microbiology, 94*(3), 223–253. https://doi.org/10.1016/j.ijfoodmicro.2004.03.022

Butnariu, M., & Bostan, C. (2011). Antimicrobial and anti-inflammatory activities of the volatile oil compounds from *Tropaeolum majus L.* (Nasturtium). *African Journal of Biotechnology, 10*(31), 5900–5909. https://doi.org/10.5897/AJB11.264

Cenci-Goga, B. T., Karama, M., Rossitto, P. V., Morgante, R. A., & Cullor, J. S. (2003). Enterotoxin production by Staphylococcus aureus isolated from mastitic cows. *Journal of Food Protection, 66*(9), 1693–1696. https://doi.org/10.4315/0362-028X-66.9.1693

Deans, S., & Ritchie, G. (1987). Antibacterial properties of plant essential oils. *International Journal of Food Microbiology, 5*(2), 165–180. https://doi.org/10.1016/0168-1605(87)90034-1

Dille, M. J., Hattrem, M. N., & Draget, K. I. (2018). Bioactively filled gelatin gels; challenges and opportunities. *Food Hydrocolloids, 76*, 17–29. https://doi.org/10.1016/j.foodhyd.2016.12.028

Evrendilek, G. A. (2015). Empirical prediction and validation of antibacterial inhibitory effects of various plant essential oils on common pathogenic bacteria. *International Journal of Food Microbiology, 202*, 35–41. https://doi.org/10.1016/j.ijfoodmicro.2015.02.030

Eysturskard, J., Haug, I. J., Ulset, A.-S., & Draget, K. I. (2009). Mechanical properties of mammalian and fish gelatins based on their weight average molecular weight and molecular weight distribution. *Food Hydrocolloids, 23*, 2315–2321. https://doi.org/10.1016/j.foodhyd.2009.06.007

Fathi-Achachlouei, B., Babolanimogadam, N., & Zahedi, Y. (2021). Influence of anise (*Pimpinella anisum L.*) essential oil on the microbial, chemical, and sensory properties of chicken fillets wrapped with gelatin film. *Food Science and Technology International, 27*(2), 123–134. https://doi.org/10.1177/1082013220935224

Fu, Y., Zu, Y., Chen, L., Efferth, T., Liang, H., Liu, Z., et al. (2007). Investigation of antibacterial activity of rosemary essential oil against *Propionibacterium acnes* with atomic force microscopy. *Planta Medica, 73*(12), 1275–1280. https://doi.org/10.1055/s-2007-981614

Garnett, J. A., Martínez-Santos, V. I., Saldaña, Z., Pape, T., Hawthorne, W., Chan, J., et al. (2012). Structural insights into the biogenesis and biofilm formation by the Escherichia coli common pilus. *Proceedings of the National Academy of Sciences, 109*(10), 3950–3955. https://doi.org/10.1073/pnas.1106733109

Goudoulas, T. B., & Germann, N. (2017). Phase transition kinetics and rheology of gelatin-alginate mixtures. *Food Hydrocolloids, 66*, 49–60. https://doi.org/10.1016/j.foodhyd.2016.12.018

Goudoulas, T. B., & Germann, N. (2019). Nonlinear rheological behavior of gelatin gels: In situ gels and individual layers. *Journal of Colloid and Interface Science, 553*, 746–757. https://doi.org/10.1016/j.jcis.2019.06.060

Hong, Y., & Brown, D. G. (2008). Electrostatic behavior of the charge-regulated bacterial cell surface. *Langmuir, 24*(9), 5003–5009. https://doi.org/10.1021/la703564q

Jafari-Sales, A., & Pashazadeh, M. (2020). Study of chemical composition and antimicrobial properties of rosemary (*Rosmarinus Officinalis*) essential oil on *Staphylococcus aureus* and *Escherichia coli* in vitro. *International Journal of Life Sciences and Biotechnology, 3*(1), 62–69. https://doi.org/10.38001/ijlsb.693371

Joly-Duhamel, C., Hellio, D., Ajdari, A., & Djabourov, M. (2002). All gelatin networks: 2. The master curve for elaticity. *Langmuir, 18*, 7158–7166. https://doi.org/10.1021/la020190m

Kim, H., Beak, S.-E., & Song, K. B. (2018). Development of a hagfish skin gelatin film containing cinnamon bark essential oil. *Lebensmittel-Wissenschaft und -Technologie-Food Science and Technology, 96*, 583–588. https://doi.org/10.1016/j.lwt.2018.06.016

Lane, D. J. (1991). 16S/23S rRNA sequencing. In E. Stackebrandt, & M. Goodfellow (Eds.), *Nucleic acid techniques in bacterial systematic* (pp. 115–175). John Wiley and Sons.

Li, X., Tu, Z.-C., Sha, X.-M., Ye, Y.-H., & Li, Z.-Y. (2020). Flavor, antimicrobial activity, and physical properties of composite film prepared with different surfactants. *Food Sciences and Nutrition, 8*, 3099–3109. https://doi.org/10.1002/fsn3.1526

Liu, Y., Lai, Q., Göker, M., Meier-Kolthoff, J. P., Wang, M., Sun, Y., et al. (2015). Genomic insights into the taxonomic status of the *Bacillus cereus* group. *Scientific Reports, 5*, 14082. https://doi.org/10.1038/srep14082

Marquis, R. E. (1968). Salt-induced contraction of bacterial cell walls. *Journal of Bacteriology, 95*(3), 775–781. https://doi.org/10.1128/JB.95.3.775-781.1968

Muthaiyan, A., Biswas, D., Crandall, P. G., Wilkinson, B. J., & Ricke, S. C. (2012). Application of orange essential oil as an antistaphylococcal agent in a dressing model. *BMC Complementary and Alternative Medicine, 12*, 1166. https://doi.org/10.1186/1472-6882-12-125

Nakagawa, S., Hillebrand, G. G., & Nunez, G. (2020). *Rosmarinus officinalis L.* (rosemary) extracts containing carnosic acid and carnosol are potent quorum sensing inhibitors

of *Staphylococcus aureus* virulence. *Antibiotics, 9*(4), 149. https://doi.org/10.3390/antibiotics9040149

Netter, A. B., Goudoulas, T. B., & Germann, N. (2020). Effects of Bloom number on phase transition of gelatin determined by means of rheological characterization. *LWT – Food Science and Technology, 132*, 109813. https://doi.org/10.1016/j.lwt.2020.109813

Ojeda-Sana, A. M., van Baren, C. M., Elechosa, M. A., Juárez, M. A., & Moreno, S. (2013). New insights into antibacterial and antioxidant activities of rosemary essential oils and their main components. *Food Control, 31*(1), 189–195. https://doi.org/10.1016/j.foodcont.2012.09.022

Osimani, A., Aquilanti, L., & Clementi, F. (2018). *Bacillus cereus* foodborne outbreaks in mass catering. *International Journal of Hospitality Management, 72*, 145–153. https://doi.org/10.1016/j.ijhm.2018.01.013

Paulo, B. B., Alvim, I. D., Reineccius, G., & Prata, A. S. (2020). Performance of oil-in-water emulsions stabilized by different types of surface-active components. *Colloids and Surfaces B: Biointerfaces, 190*, 110939. https://doi.org/10.1016/j.colsurfb.2020.110939

Poppe, J. (1992). Gelatin. In *Thickening and gelling agents for food* (pp. 98–123). Springer.

Rodríguez-Rojo, S., Varona, S., Núñez, M., & Cocero, M. J. (2012). Characterization of rosemary essential oil for biodegradable emulsions. *Industrial Crops and Products, 37*, 137–140. https://doi.org/10.1016/j.indcrop.2011.11.026

Salehi, B., Sharopov, F., Tumer, T. B., , … Cho, W. C., & Martins, N. (2019). *Symphytum* species: A comprehensive review on chemical composition, food applications and phytopharmacology. *Molecules, 24*(12), 2272. https://doi.org/10.3390/molecules24122272

Schneiderheinze, J. M., Armstrong, D. W., Schulte, G., & Westenberg, D. J. (2000). High efficiency separation of microbial aggregates using capillary electrophoresis. *FEMS Microbiology Letters, 189*(1), 39–44. https://doi.org/10.1016/S0378-1097(00)00249-4

Schneider, C. A., Rasband, W. S., & Eliceiri, K. W. (2012). NIH image to ImageJ: 25 years of image analysis. *Nature Methods, 9*(7), 671–675. https://doi.org/10.1038/nmeth.2089

Sikkema, J., De Bont, J. A. M., & Poolman, B. (1995). Mechanisms of membrane toxicity of hydrocarbons. *Microbiological Reviews, 59*(2), 201–222. https://doi.org/10.1128/mmbr.59.2.201-222.1995

Sun, W., Huang, L., Yang, Y., Liu, X., & Tong, Z. (2015). Large amplitude oscillatory shear studies on the strain-stiffening behavior of gelatin gels. *Chinese Journal of Polymer Science, 33*(1), 70–83. https://doi.org/10.1007/s10118-015-1559-5

Taylor, J. M., Tomlins, P., & Sahota, T. S. (2017). Thermoresponsive gels. *Gels, 3*, 4. https://doi.org/10.3390/gels3010004

Tongnuanchan, P., & Benjakul, S. (2014). Essential oils: Extraction, bioactivities, and their uses for food preservation. *Journal of Food Science, 79*(7), R1231–R1249. https://doi.org/10.1111/1750-3841.12492

Vardanian, A., Kurzbaum, E., Farber, Y., Butnariu, M., & Armon, R. (2018). Facilitated enumeration of the silicate bacterium *Paenibacillus mucilaginosus* comb. nov. (formerly *Bacillus mucilaginosus*) via tetrazolium chloride incorporation into a double agar-based solid growth medium. *Folia Microbiologica, 63*(3), 401–404. https://doi.org/10.1007/s12223-017-0567-y

Weiss, J., Loeffler, M., & Terjung, N. (2015). The antimicrobial paradox: Why preservatives lose activity in foods. *Current Opinion in Food Science, 4*, 69–75. https://doi.org/10.1016/j.cofs.2015.05.008

Wu, J., Liu, H., Ge, S., Wang, S., Qin, Z., Chen, L., et al. (2015). The preparation, characterization, antimicrobial stability and in vitro release evaluation of fish gelatin films incorporated with cinnamon essential oil nanoliposomes. *Food Hydrocolloids, 43*, 427–435. https://doi.org/10.1016/j.foodhyd.2014.06.017

Yashaswini, P., & Arvind. (2018). Antimicrobial properties of orange (*Citrus reticulata* var. *Kinnow*) peel extracts against pathogenic bacteria. *International Journal of Current Microbiology and Applied Sciences, 7*, 737–746. https://doi.org/10.20546/ijcmas.2018.703.086

Zhang, T., Ding, M., Tao, N., Wang, X., & Zhong, J. (2020). Effects of surfactant type and preparation pH on the droplets and emulsion forms of fish oil-loaded gelatin/surfactant stabilized emulsions. *Lebensmittel-Wissenschaft und -Technologie- Food Science and Technology, 117*, 108654. https://doi.org/10.1016/j.lwt.2019.108654

Zhang, T., Ding, M., Wang, X., & Zhong, J. (2020). Droplet and creaming stability of fish oil-loaded gelatin/surfactant-stabilized emulsions depends on both the adsorption ways of emulsifiers and the adjusted pH. *Food Science and Human Wellness, 9*(3), 280–288. https://doi.org/10.1016/j.fshw.2020.04.0022